Age and growth of striped marlin (*Kajikia audax*) in the Southwest Pacific Ocean

R. Keller Kopf[1]*, Peter S. Davie[2], Donald Bromhead[3], and Julian G. Pepperell[4]

[1]*Institute for Land, Water and Society, Charles Sturt University, PO Box 789, Albury, NSW 2640, Australia*
[2]*Institute of Veterinary Animal and Biomedical Sciences, Massey University, Private Bag 11 222, Palmerston North, New Zealand*
[3]*Oceanic Fisheries Programme, Secretariat of the Pacific Community, BP D5, 98848 Noumea Cedex, New Caledonia*
[4]*Pepperell Research and Consulting Pty Ltd, PO Box 1475, Noosaville DC, QLD 4566, Australia*

Corresponding Author: tel: +61 2 6051 9294; fax: +61 2 6051 9897; e-mail: rkopf@csu.edu.au.

This study describes the first validated model of age and growth developed for striped marlin (*Kajikia audax*). Daily periodicity of otolith microincrements was corroborated by back-calculated hatch dates that matched the known spawning season in the Southwest Pacific Ocean (SWPO). Yearly annulus formation in fin-spine sections was corroborated by daily otolith microincrements and by a marginal increment analysis. Ages of females ranged from 140 d to 8.5 years in fish between 990 mm and 2872 mm lower-jaw fork length (LJFL), and ages of males from 130 d to 7.0 years in fish between 1120 mm and 2540 mm LJFL. Sex-specific differences in growth were significant, with females growing to a larger asymptotic size and greater age than males. An instantaneous growth rate of 3.1 mm d^{-1} at 6 months and an estimated length of 1422–1674 mm LJFL by age 1 year makes this species among the fastest growing bony fish. Implications of these findings are discussed in relation to commercial longline and recreational fisheries management of striped marlin in the SWPO and in relation to the biology of pelagic fish growth.

Keywords: body size, *Kajikia audax*, life history, sclerochronology, stock assessment, tuna and billfish.

Introduction

The striped marlin (*Kajikia audax*; Collette *et al.*, 2006) is an apex predator in the open ocean of the Indo-Pacific (Revill *et al.*, 2009) and is valued in commercial longline and recreational fisheries throughout its distribution (Dalzell and Boggs, 2003; Bromhead *et al.*, 2004). It is highly migratory and broadly distributed across tropical, subtropical, and temperate oceanic waters (Nakamura, 1985). Differences in genetic population structure (McDowell and Graves, 2008), body size (Squire and Suzuki, 1990; Kopf *et al.*, 2005), movement patterns (Domeier, 2006; Sippel *et al.*, 2007; Holdsworth *et al.*, 2009), and spawning dynamics (Hanamoto, 1977; Kopf, 2010) suggest the existence of a semi-independent stock in the Southwest Pacific Ocean (SWPO; 0–40°S 145°E–130°W).

There is a need to assess the sustainability of fishing practices for striped marlin in the SWPO and globally. However, the feasibility of estimating stock productivity and current status is hindered by a lack of validated age information needed to estimate growth parameters, mortality schedules, and age-at-maturity (Langley *et al.*, 2006; Brodziak and Piner, 2010). Annual commercial longline catch of striped marlin in the SWPO has declined from a peak of >12 000 t in the early 1950s to <2500 t annually since the 1990s (Bromhead *et al.*, 2004; Langley *et al.*, 2006). Several thousand striped marlin are tagged and released in a typical year within recreational fisheries of Australia and New Zealand (Holdsworth *et al.*, 2003; Bromhead *et al.*, 2004).

Preliminary stock assessment scenarios for the SWPO suggest that this species has been harvested at a level close to, or above, the spawning biomass required to support maximum sustainable yield (Langley *et al.*, 2006). Until the estimates of stock status can be determined with greater certainty, the Western and Central Pacific Fisheries Commission (WCPFC) has put in place a Conservation and Management Measure (2006-04) that limits the number of vessels fishing for striped marlin. Stock modelling of North Pacific striped marlin also suggests overharvesting (Brodziak and Piner, 2010), and the International Scientific Committee (ISC) has issued similar fisheries restrictions (ISC, 2010).

Methods used to estimate the age of striped marlin have not been validated, and previous estimates of growth vary widely (Koto, 1963; Skillman and Yong, 1976; Davie and Hall, 1990; Melo-Barrera *et al.*, 2003; Kopf *et al.*, 2005). Age validation in billfish (Istiophoridae, Xiphiidae) is complicated by the significant expense and time required to collect samples from large-bodied, migratory, solitary species that inhabit the open ocean (Holland, 2003). Chemical mark–recapture age-validation studies have had limited success owing to low recapture rates of <0.93% in striped marlin (Speare, 1992, 2003; Ortiz *et al.*, 2003). Methodological difficulties associated with age estimation, including vascularization of the fin-spine core, interpretation of annuli, and the small size of otoliths, have also hindered progress in age validation and growth modelling of billfish (Kopf *et al.*, 2010).

The aim of our study was to address some of the limitations of previous age and growth studies on striped marlin by testing multiple age-validation techniques and by sampling widely across the

distribution and demographic structure of the stock in the SWPO. The objectives of the research were to (i) determine the periodicity of microincrement formation in sagittal otoliths, (ii) identify the age at which the first translucent zone was formed in fin-spines, (iii) determine the periodicity and seasonal timing of formation of the translucent zone in fin-spines, and (iv) develop a sex-specific growth model for striped marlin in the SWPO.

Methods

Paired sagittal otoliths ($n = 193$) and first dorsal and anal fin-spines ($n = 425$) were collected from striped marlin caught in the SWPO between January 2006 and January 2009 (Table 1, Figure 1). Lower-jaw fork length (LJFL, mm), eye-fork length (EFL, mm), whole weight (kg), sex, date, method of capture, and location (latitude and longitude or approximate area) were recorded. Fin-spines and otoliths were collected at recreational fishing competitions in New South Wales, Australia, Northland, New Zealand, and at sea on commercial longliners fishing off the east coast of Australia, Fiji, New Caledonia, and French Polynesia. Samples from Fiji, New Caledonia, and French Polynesia are referred to collectively as Pacific Island Countries and Territories (PICTs). First dorsal fin-spines 1–6 (D1–6) and first anal fin-spines 1–3 (A1–3) were excised with the condyle intact. Fin-spines were cleaned, dried, and stored following the methods described by Kopf *et al.* (2010). Otoliths were extracted from frozen head sections following Radtke (1983) and were cleaned with distilled water and dried at room temperature for 24 h. Sex was verified in 83% (354 of 425) of striped marlin by gonad histology, 15% (63 of 425) by macroscopic examination, and remained undetermined in 2% (8 of 425) of the samples.

Fin-spine annulus counts

Maximum condyle width (CW) of fin-spine D4 was measured (± 0.01 mm), and transverse sections 0.3–0.6 mm thick were cut at a level of 1/4 CW using a lapidary saw (Figure 2). Fin-spine D4 at section level 1/4 CW was the most suitable

section for age estimation because it was the least vascular and showed the greatest number of clear annuli (Kopf and Davie, 2011). Fin-spines D5 and D6 and A3 at level 1/4 CW−1 CW were interchangeable (Kopf and Davie, 2011) and were used in this study when D4, 1/4 CW was unavailable. Digital images of slide-mounted sections and separate images of the marginal increment were captured under reflected light at magnifications of ×4–100 using a DP-170 Olympus camera attached to a BX51 Olympus light microscope. Measurements (± 0.01 mm) were made between the focus and the radius of the vascularized area, section radius, annulus radius, and width of the marginal increment (Figure 2A–F). Annulus radius was measured from the focus to the outer edge of each translucent zone. The marginal increment was the straight-line distance between the outer edge of the last translucent zone and the edge of the fin-spine section (Figure 2). Measurements were recorded from digital images using free public-domain software, Image J version 1.32 (Rasband, 1997–2008).

A putative yearly/seasonal annulus was defined as a wide opaque zone followed by a narrow translucent one (Panfili *et al.*, 2002). Narrow translucent zones were demarcated on digital images for age determination and annulus measurements because they represented the presumed endpoint of a yearly structure (Figure 3). Age estimates were assigned based on the total number of paired opaque and translucent zones, referred to hereafter as "annuli". Annulus criteria were consistent with studies on billfish (Hill *et al.*, 1989; Speare, 2003; DeMartini *et al.*, 2007; Kopf *et al.*, 2010) and other teleost fish (Panfili *et al.*, 2002). False doublet and triplet increments (Figure 3) were counted as a single annulus when the width between translucent zones increased by >25% over the previous zone. False increments were not counted if the translucent zone failed to extend into the cranial or caudal margin of the section (Speare, 2003) or if the translucent zone was faint, thin, or segmented (DeMartini *et al.*, 2007).

All fin-spine sections ($n = 425$) were read twice by the primary reader. An external reader at the Central Ageing Facility (CAF) in

Table 1. Number (n) and mean length (LJFL, mm) of female and male striped marlin ($n = 425$) sampled during each quarter of the year in the SWPO.

Quarter	Year	Female			Male		
		n	Mean LJFL	s.d.	n	Mean LJFL	s.d.
1	2005[a]	–	–	–	1	1 860	–
	2006	56	2 384	154	34	2 319	146
	2007	30	2 350	172	25	2 248	108
	2008	12	2 250	99	26	2 191	149
2	2005	1	2 710	–	–	–	–
	2006	6	2 495	40	3	2 195	191
	2007	26	2 382	97	19	2 211	346
	2008	14	1 644	515	15	1 978	395
3	2006	–	–	–	1	2 200	–
	2007	2	2 325	361	12	1 991	135
	2008	6	2 207	163	5	2 136	113
4	2006	18	2 230	272	18	2 187	132
	2007	23	2 326	226	42	2 094	175
	2008	12	2 390	136	10	2 153	106
Total[b]		206	2 300	281	211	2 170	219

[a]Two fin-spine samples from 2005 were included in the analyses because of the lack of samples <1900 mm and >2700 mm LJFL.
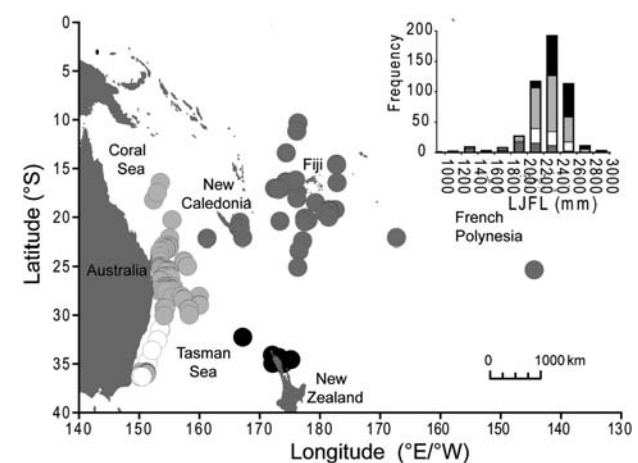[b]The sex of eight fish was not determined.

Figure 1. Map of the SWPO showing the locations of the striped marlin ($n = 425$) sampled and the length frequency distribution for each fishery. Fisheries included are the Australian commercial longline (light grey; AUS COMM), the Australian recreational (white; AUS REC), the New Zealand recreational (black; NZ REC), and the longline fisheries from PICTs (dark grey; PICT COMM).
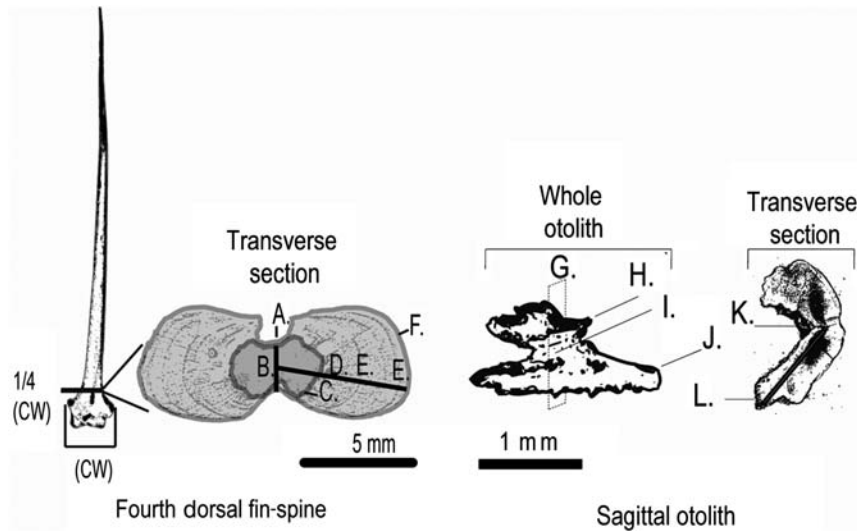
Figure 2. Fourth dorsal fin-spine and sagittal otolith of a striped marlin alongside respective transverse sections. Notable features of the dorsal fin-spine include maximum CW and in transverse section (A) vertical axis, (B) focus, (C) vascularized perimeter, (D) horizontal axis/annulus counting path/measurement axis, (E) translucent zone, and (F) perimeter. The marginal increment was measured as the straight-line distance between the edge of the last translucent zone and the perimeter of the fin-spine section. Features of a whole sagittal otolith including (G) the transverse plane used for microincrement counts, (H) antirostrum, (I) primordium, and (J) rostrum. The transverse section shows the microincrement counting path (grey line) between the (K) primordium and (L) edge of the ventral lobe.

Queenscliff, Australia, read all sections processed by mid-2008 (81%; 346 of 425). Readings were conducted at least 1 month apart using digital images, without scale bars, or other identifiable features. Digital images were used to make annulus counts during readings, but microscope slide sections were re-examined if there was a discrepancy. If discrepancies between readings or readers could not be resolved, the section was considered unreadable and discarded.

Final age estimates were based on the number of annuli counted outside the vascularized area (Yatomi, 1990; Drew *et al.*, 2006), plus the number of annuli replaced through vascular erosion of the fin-spine core (Hill *et al.*, 1989). Half-year (+0.5) ages were assigned if the marginal increment/edge type was greater than half the width of the previous opaque zone (Kopf *et al.*, 2010). Following methods described by Hill *et al.* (1989), annuli lost through vascularization were identified using the measurements of fin-spine sections from small/young striped marlin unaffected by vascularization.

Otolith microincrement counts

Otoliths were fixed to a laser-cut microscope slide using thermoplastic glue (Crystal Bond 508) and positioned so that the edge of the slide passed directly through the primordium in transverse plane (Figure 2G). Otoliths were checked under a light microscope to ensure that the edge of the slide passed squarely through the primordium, with the antirostrum and rostrum protruding over the edge (Figure 2H and J). If the otolith was not aligned squarely, then the thermoplastic glue was reheated and the process repeated. A transverse section was produced by grinding the overhanging rostrum and antirostrum flush against the edge of the slide with 500-grit wet/dry sandpaper. Once the primordium (edge of the slide) was reached, the surface was polished with 1000-grit wet/dry sandpaper then with 3 µm alum powder. The thermoplastic glue was reheated and the polished surface of the otolith was

placed face down on the centre of the slide. The unpolished surface was ground to ~50 µm thick using 500 and 1000-grit wet/dry sandpaper. A microscope coverslide 50 µm thick was placed on either side of the section to prevent overgrinding and to ensure consistent thickness. The section was viewed under a light microscope at ×20–40 magnification and polished using 3 µm alum powder. The section was polished and photographed until microincrements could be resolved from the primordium out to the edge of the ventral lobe (Figure 2K and L).

Presumed daily microincrement counts were made on 28 otoliths from juvenile or young adult striped marlin. The counting path extended from the primordium to the edge of the ventral lobe, which also served as the measurement axis for otolith radius (± 1.0 µm; Figure 2). Primary increments, as detailed by Brothers *et al.* (1983) and Prince *et al.* (1991), were counted. Estimates based on subcounts followed methods described by Ralston and Williams (1988) and included widths of 10–30 microincrements averaged and multiplied across the distance of the unclear area. Each section was read twice, and the mean of the two counts was used as the final age estimate.

Statistical analysis

Differences in linear regressions were evaluated by overall tests of coincidental regression (Zar, 1999), and differences in non-linear relationships were evaluated by analysis of the residual sum of squares (ARSS; Chen *et al.*, 1992). The relationships between LJFL and section radius (mm) of fin-spine D4, 1/4 CW, and otolith section radius (µm) were evaluated by power functions (Ehrhardt, 1992) and standard linear functions with intercepts determined by regression or fixed at the origin (Zar, 1999). Assumptions of normality and constant variance of residuals in regressions were evaluated, and variables were logtransformed or ranked when necessary. The precision of annulus counts and microincrement counts was assessed using average per cent error
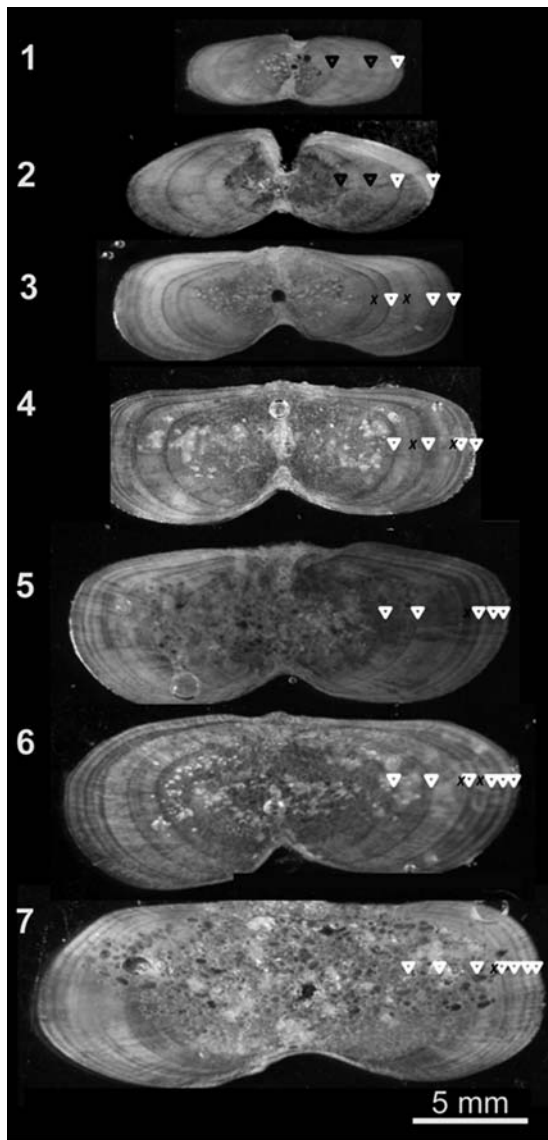
Figure 3. Images of typical dorsal fin-spine sections from striped marlin in the SWPO. Illustrations show annulus counts (white triangles), false increments (black crosses), and annuli replaced because of vascularization of the core. False annuli corroborated by otolith daily microincrement counts are denoted by black triangles.

(APE; Beamish and Fournier, 1981). Differences in median length and age were evaluated using a Mann–Whitney rank-sum test (M–W RNK SUM) or Kruskal–Wallis one-way ANOVA on ranks (K–S ANOVA RKS) with *post hoc* comparisons following Dunn's method (Zar, 1999).

Corroboration of daily microincrement periodicity

Hatch dates of striped marlin were back-calculated by subtracting daily microincrement counts from the date of capture (Prince *et al.*, 1991). Striped marlin in the SWPO spawn during the austral spring or early summer, between 1 September and 31 January (Hanamoto, 1977; Kopf, 2010). If microincrements were not related to daily age, then the proportion of back-calculated hatch dates falling within the spawning period was assumed to be equal to, or less than, the number of hatch dates predicted to

fall outside the spawning period. Proportions of back-calculated hatch dates were compared using Chi-squared analyses of contingency tables (Zar, 1999), based on potential microincrement periodicities of one, two, and 0.5 microincrements per day. Fisher's exact tests employing the binomial coefficient were used in *post hoc* comparisons (Zar, 1999).

Validation of age at first annulus formation

Age (d) at first annulus formation in fin-spine sections was identified by comparing otolith microincrement counts with matching sets of fin-spines from juvenile and young adult striped marlin ($n = 28$). The relationship between fin-spine section radius and estimated otolith age (d) was described by the two-parameter exponential growth equation Age (d) $= a[e^{(bSR)}]$, where SR is the spline radius (mm) and variables a and b are fitted parameters.

To predict the age (d) at first annulus formation, the above growth equation was compared with the frequency distribution of the first annulus ($n = 299$). This approach was adapted from methods used to predict the location of the first annulus described by Campana (2001) and DeMartini *et al.* (2007). The observed frequency distribution of the first annulus ($n = 299$) was fitted to a Gaussian peak regression equation with variables a and b as fitted parameters, and c as the modal radius at first annulus formation. The modal radius at first annulus formation was used in the exponential growth regression model to predict the age (d) at first annulus formation. Median age (d) and the radius of the first annulus were compared between the daily aged subsample ($n = 28$) and all fin-spine sections ($n = 299$) using an M–W RNK SUM test.

Validation of annulus periodicity

The periodicity and timing of translucent zone formation was determined using a marginal increment analysis (MIA; Campana, 2001). The marginal increment ratio (MIR) was described by the equation (Prince *et al.*, 1988) MIR $= (SR - r_n)/(r_n - r_{n-1})$. The variable SR is the spine radius (mm), r_n the radius (mm) of the last annulus, and r_{n-1} the radius (mm) of the penultimate annulus. Annulus radius measurements extended from the focus to the outside edge of each translucent zone.

To test the hypothesis of a single 12-month cycle of annulus formation, monthly MIRs were fitted to the three-parameter Gaussian peak regression equation MIR $= a[e^{(-0.5\ SR\ -\ c/b)}]^2$. Here, the variables a and b are fitted parameters, and c is the month at which the MIR peaks. A two-way ANOVA (TW ANOVA) on ranks (Zar, 1999) was used to compare yearly and monthly differences in MIRs between presumed age groups 2–3, 4–8.5, and all ages combined for males and females. Ranked MIRs could not be compared *post hoc* because overlapping rank sums violated statistical assumptions. Therefore, the timing of annulus formation was compared statistically by grouped quarterly values using Dunn's method (Zar, 1999). To ensure consistency in margin measurements, the MIA was restricted to fin-spine sections ($n = 352$) more than 1-year old, where the margin was classified as readable, and where spines D4–6 or A3 were sectioned at 1/4 CW or 1 CW.

Daily growth

Daily otolith age and LJFL of striped marlin was described by the three-parameter Gompertz regression equation LJFL$_d = a\,e[-e^{-(d\ -\ c/b)}]$, where LJFL$_t$ is the length (mm) at daily otolith age d, d the daily otolith age, c the otolith age (d) at

hypothetical length zero; and a and b the fitted parameters. Length-at-age 1 and 2 estimated by otolith microincrement counts and by fin-spine annulus counts were compared using an M−W RNK SUM test (Zar, 1999).

Annual growth

Growth of male and female striped marlin was modelled from observed and back-calculated LJFL-at-age estimates. Back-calculation techniques were evaluated to estimate the LJFL-at-age of small (>1750 mm LJFL) fish underrepresented in the sample collection. Back-calculated LJFL-at-age was estimated using a standard linear Dahl−Lea (Back-calculation 1), modified linear Dahl−Lea (Back-calculation 2), and a modified non-linear Fraser−Lee method (Back-calculation 3). The standard linear Dahl−Lea/Back-calculation 1 was described by the equation (Panfili et al., 2002) $LJFL_t$ (mm) = $(LJFL/SR)SR_t$. The modified linear Dahl−Lea/Back-calculation 2 was described by the equation (Francis, 1990) $LJFL_t$ (mm) = $LJFL(a + b\,SR_t)/(a + b\,SR)$. The modified non-linear Fraser−Lee/Back-calculation 3, previously developed for swordfish (Xiphias gladius), was described by the equation (Ehrhardt, 1992) $\log LJFL_t$ (mm) = $L \log a + [\log SR_t$ $(\log LJFL - \log a)/\log SR]$, where $LJFL_t$ is the length (mm) at yearly age t, SR_t the annulus radius (mm) at yearly age t, LJFL the observed length (mm) at capture, SR the observed spine radius (mm) at capture, and a and b the fitted parameters.

The standard Dahl−Lea methodology assumed direct proportionality, with intercepts passing through the origin, and the parameters a and b of the modified Dahl−Lea method were determined by linear regression of the fin-spine radius and LJFL relationship. Parameter a in the modified Fraser−Lee method was determined from the logarithm of the direct proportionality parameter of the power function fitted to the fin-spine radius and LJFL relationship. Back-calculation techniques were restricted to samples where the fourth dorsal (D4) fin-spine was available and where the section was cut at 1/4 CW ($n = 299$). Suboptimal spines D5 and D6 and A3, 1/4 CW−1 CW ($n = 75$) were excluded from back-calculation techniques because of possible allometric differences.

Growth was modelled using a standard (von Bertalanffy, 1938) and generalized von Bertalanffy growth curve (VBGC; Richards, 1959). The VBGCs were fitted to observed and three back-calculated LJFL-at-age datasets, which were compared with previous VBGCs developed for striped marlin (Skillman and Yong, 1976; Melo-Barrera et al., 2003; Kopf et al., 2005). Skillman and Yong (1976) reported that weights were converted to fork length (FL), "tip of bill to middle point on posterior margin of middle caudal fin rays". This measurement was assumed equivalent to the FL reported by Nakamura (1985) and was transformed to LJFL using the conversion developed for striped marlin in SWPO (Kopf, 2010): FL = a LJFL + b, where $a = 1.067$ and 1.021 and $b = 192.85$ and 319.35 for females and males, respectively.

Observed LJFL-at-age was fitted using the Gauss−Newton non-linear procedure in SAS (SAS Institute, 1990). To eliminate the bias associated with autocorrelation, back-calculated growth histories were fitted using a non-linear repeated-measures algorithm (Jones, 2000). The standard VBGC was described by the equation (von Bertalanffy, 1938) $LJFL_t = L_\infty[1 - e^{-k(t-t_0)}]$. The generalized VBGC was described by the equation (Richards, 1959) $LJFL_t = L_\infty\left[1 - e^{-K(1-m)(t-t_0)}\right]^{(1/(1-m))}$, where $LJFL_t$ is the mean length at age t, L_∞ the asymptotic length, k and K the growth

coefficients, t the age (years), t_0 the age (years) at hypothetical length zero, and m the fitted fourth parameter in the generalized function.

Results

Corroboration of daily microincrement periodicity

Daily periodicity resulted in a significantly greater proportion (25 of 28) of back-calculated hatch dates (Table 2) falling within the spawning period compared with potential periodicities of two (Fisher's exact test; 18 of 28; $p = 0.03$) and 0.5 (Fisher's exact test; 7 of 28; $p < 0.001$) microincrements formed per day. The proportion of back-calculated hatch dates within and outside the spawning period were significantly different (χ^2; $p < 0.001$). Potential periodicity of two microincrements per day was not significantly different from parity (Fisher's exact test; $p = 0.42$).

Daily microincrement counts ranged from 130 to 630 d, with decreasing precision between lengths of 990 and 2140 mm LJFL (Table 2). The precision of microincrement counts was 7.5% APE. The APE equated to 9 ± 6 d in sections aged <1 year, and 34 ± 36 d for all sections combined. Error ($\pm$) values are reported as standard deviations (s.d.), unless otherwise stated. Otolith section radius increased linearly ($r^2 = 0.61$; $p < 0.001$) with LJFL, and there were no significant sex-specific differences (Table 3). The mean microincrement count for both sexes combined was 385 ± 42 d over a mean LJFL of 1586 ± 62 mm (∼27 kg). Microincrements were confidently enumerated up to a mean of 436 ± 14 d or 1710 mm LJFL. Beyond that age and size, more than half the microincrements were estimated using the subcount method. Therefore, otolith microincrement counts were not considered suitable for validating the age of the second annulus. The width of microincrements declined progressively to <0.99 μm at 436 d.

Validation of the first annulus and yearly annulus formation

Radius measurements ranged from a mean of 5.35 ± 0.62 mm at annulus 1 to 11.34 ± 0.07 mm at annulus 8 (Figure 4). An exponential growth model ($r^2 = 0.72$; $p < 0.001$) was fitted to the relationship between fin-spine section radius and daily age (Table 3). The radius of the first annulus ranged from 4.38 to 6.31 mm, with a modal frequency predicted at 5.27 ± 0.58 mm (Figure 5). The predicted age at first annulus formation was 301 ± 119 d. False annuli before the first yearly annulus were identified by otolith daily microincrements and were observed at a radius of 1.1−1.6 mm and 2.3−3.3 mm in 16% (47 of 299) of the fin-spines examined. Daily estimates of age suggested that false annuli formed at ∼83 and 128 d after hatching. There were no significant differences in the median radius of the first annulus between sexes (M−W RNK SUM; $p = 0.44$) or between the daily aged sample and all fin-spine sections (M−W RNK SUM; $p = 0.28$).

The pattern of annulus deposition (Figure 6) conformed to a single 12-month cycle of periodicity and did not differ between sexes ($r^2 = 0.65$; $p < 0.001$). In all, 16 immature striped marlin sampled during the spawning season had at least one complete annulus. The width of opaque zones increased during the first and the second quarters of the year, and translucent zones were completed during the fourth quarter (Figure 6). The Gaussian regression equation for combined samples predicted a peak MIR of 0.43 during June. Combined age groups and years showed

Table 2. Daily microincrement counts from sagittal otoliths of striped marlin ($n = 28$) caught in the SWPO between 2006 and 2009, with catch information including LJFL, whole weight (kg), and location (latitude and longitude), and precision estimates calculated using APE.

Estimated age (d)	Precision APE ($\pm$ d)	Length (mm, LJFL)	Estimated[a] weight (kg)	Sex	Latitude and longitude	Hatch date (dd mm yyyy)
140	4	990	4	F	18.1°S 176.2°E	23 December 2007
130	7	1 120	7	M	20.5°S 173.4°E	19 December 2006
160	2	1 130	7	F	18.1°S 176.2°E	3 December 2007
170	4	1 220	9	M	17.1°S 172.6°E	28 October 2007
163	4	1 230	9	M	17.1°S 173°E	1 November 2007
192	7	1 290	11	M	17.2°S 173.2°E	6 October 2007
176	14	1 320	12	F	17.1°S 172.5°E	19 October 2007
181	19	1 320	12	F	17.1°S 173.6°E	17 October 2007
158	8	1 330	12	F	17.1°S 172.5°E	6 November 2007
200	20	1 350	12[b]	F	25.1°S 154.1°E	16 September 2007
216	12	1 410	15	F	16.2°S 176°E	24 September 2007
208	10	1 420	16	F	16.2°S 176°E	2 October 2007
383	21	1 490	21[b]	M	25.6°S 154.6°E	4 November 2006
366	14	1 640	24[b]	F	30°S 158.4°E	7 December 2005
429	30	1 703	30	F	27.4°S 155.5°E	5 September 2005
309	27	1 740	32	–[c]	25.1°S 176.4°E	12 October 2006
480	9	1 770	34	M	36°S 150.3°E	21 December 2005
344	45	1 770	34	F	18.6°S 179.3°E	26 October 2006
590	88	1 850	40	M	20.5°S 177.6°E	11 January 2006
868	34	1 910	45	M	14.7°S 177.2°W	4 June 2005
731	39	1 910	45	M	19.5°S 178.5°W	24 October 2005
682	73	1 920	46	M	20.1°S 178.5°W	14 November 2005
627	161	1 930	47	M	20.1°S 177.5°E	7 December 2005
649	73	1 930	47	M	16.4°S 174.4°E	27 January 2006
640	40	1 970	50	M	27.4°S 154°E	14 November 2005
616	50	1 980	51	M	29°S 160°E	6 March 2005
562	41	2 000	53	M	11.2°S 176.2°E	19 January 2006
630	98	2 140	67	F	27.5°S 153.4°E	20 March 2005

Estimated hatch dates were back-calculated by subtracting daily microincrement count from the date of capture.
[a]Weight estimated using the regression equations in Table 3.
[b]Weight (kg) measured directly.
[c]Sex not determined.

Table 3. Regression models and daily growth equations developed for striped marlin in the SWPO between 2006 and 2009.

Model	Equation	Sex	r^2	n	a	b	c
LJFL (mm) and EFL (mm)	EFL $= a$ LJFL $+ b$	Both	0.95	301	0.834	36.61	–
		Female	0.96	136	0.838	23.75	–
		Male	0.94	159	0.827	49.83	–
LJFL (mm) and whole weight (kg)	Weight $= a$ LJFL^b	Both	0.93	214	1.012×10^{-10}	3.55	–
		Female	0.95	120	4.171×10^{-11}	3.67	–
		Male	0.89	89	1.902×10^{-9}	3.16	–
Spine radius (mm) and LJFL (mm)	LJFL $= a$ SR^b	Both	0.84	299	432.93	0.77	
	LJFL $= a$ SR $+ b$	Both	0.8	299	191.8	622.43	–
Otolith radius (μm) and LJFL (mm)	LJFL $= a$ OR $+ b$	Both	0.61	28	1.727	6.49×10^{-2}	–
Age (d) and spine radius (mm)	Age $= a[e^{(bsR)}]$	Both	0.72	28	50.49	0.339	–
MIR and month	MIR $= ae(-0.5$ month $- c/b)^2$	Both	0.65	352	0.441	4.61	6.4
Age (d) and LJFL (mm)	LJFL$_d = ae[-e^{-(d-c/b)}]$	Both	0.92	28	1 999.013	177.97	37

significant differences in MIR values between months for females (TW ANOVA RKS; $p < 0.001$), males (TW ANOVA RKS; $p < 0.001$), and combined-sexes age group $2-3$ (TW ANOVA RKS; $p < 0.01$), but not age group $4-8.5$. Quarterly marginal increment values peaked at 0.42 during the austral winter and dropped to their lowest value of 0.20 during the austral spring. The median MIR during the fourth quarter was significantly less than during the third and second quarters of the year (Dunn's; $p < 0.05$).

Age and growth

The lengths of female striped marlin ranged from 990 mm (4 kg) to 2872 mm (168 kg), and age estimates from 140 d to 8.5 years.

Lengths of male striped marlin ranged from 1120 mm (7 kg) to 2540 mm (122 kg), and age estimates from 130 d to 7.0 years. The APE of annulus counts made by the primary reader was 9.8%, and the APE between ageing laboratories was 13.7%. In all, 12% (51 of 425) of fin-spine sections were unreadable and excluded from growth analyses. The remaining 374 sections were used in growth analyses, but back-calculation techniques were restricted to 299 sections from the optimal spine (D4) and section level (1/4 CW). Vascularization affected 27% of readable fin-spine sections, whereby $1-3$ annuli were estimated to have been reabsorbed. Vascularization affected annuli in fish as young as 1.5 years or ~1976 mm LJFL.
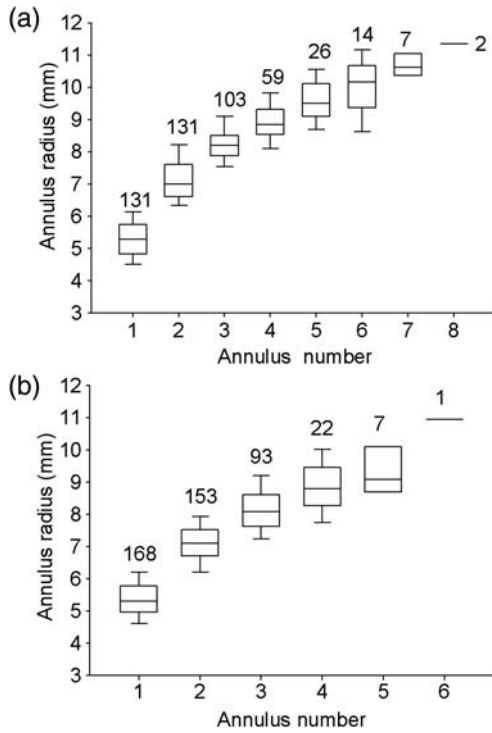
Figure 4. Box plots of annulus radius (mm) for first dorsal fin-spine four, level one-fourth CW of (a) female and (b) male striped marlin ($n = 299$). The horizontal line in each box plot represents the median annulus radius, and the boundaries represent 25th and 75th percentiles.
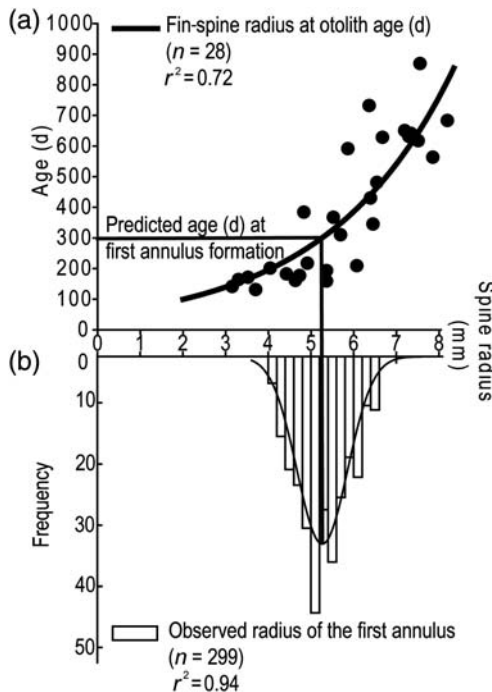

Figure 5. Daily age at first annulus formation estimated for striped marlin in the SWPO including (a) relationship between otolith age and fin-spine section radius, and (b) observed frequency distribution of first annulus radius. The drop-line illustrates the predicted age (301 ± 119 d) at first annulus formation.
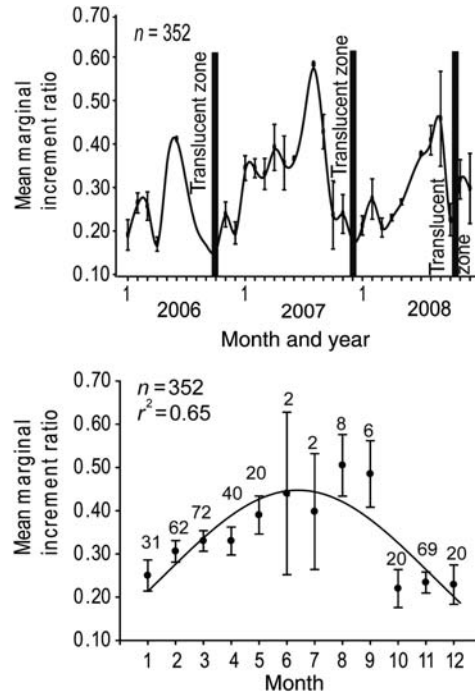
Figure 6. Mean MIR ($\pm 95\%$ confidence intervals) by month for striped marlin sampled in the SWPO between 2006 and 2009. The bottom panel illustrates combined years fitted to the Gaussian peak regression, and the top panel a running average across years.
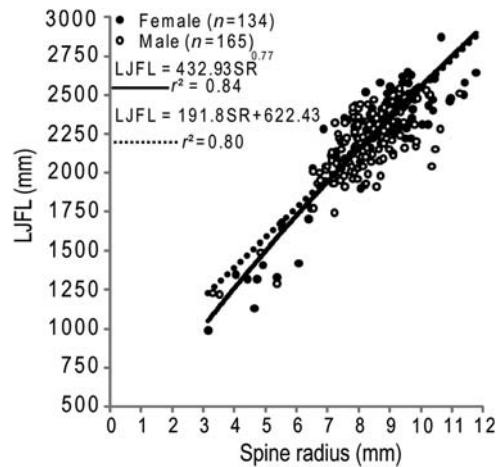

Figure 7. Power (solid line) and linear (broken line) functions fitted to the observed fin-spine radius and LJFL of striped marlin.

Combined-sex power ($r^2 = 0.84$) and linear functions ($r^2 = 0.80$) were used in back-calculation models to describe the fin-spine radius and LJFL relationship (Figure 7). Functions with the intercept fixed at the origin resulted in lower coefficients of determination and did not pass through datapoints for small striped marlin (<1750 mm LJFL). The standard VBGC was fitted successfully to observed and three back-calculation models for each sex (Figure 8, Table 4). The generalized VBGC failed to converge on a value in all models unless parameter constraints were applied, or if the model was applied to mean LJFL-at-age. For that reason, growth was modelled using the standard VBGC only.
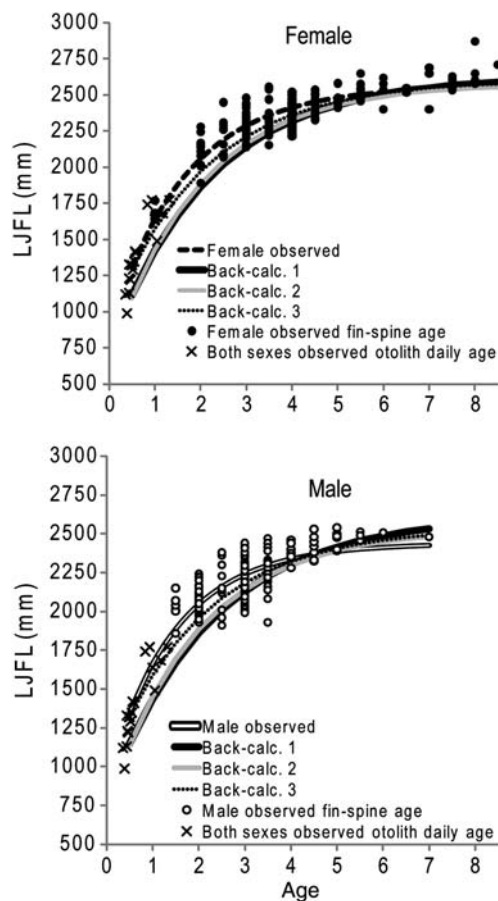
Figure 8. Standard VBGCs and parameters estimated for (top) female and (bottom) male striped marlin in the SWPO. Growth parameters of females and males, respectively, were fitted to: observed ($L_\infty = 2565$, $k = 0.60$, $t_0 = -0.70$; $L_\infty = 2438$, $k = 0.68$, $t_0 = -0.69$); back-calculation 1 ($L_\infty = 2628$, $k = 0.46$, $t_0 = -0.71$; $L_\infty = 2615$, $k = 0.44$, $t_0 = -0.81$); back-calculation 2 ($L_\infty = 2580$, $k = 0.51$, $t_0 = -0.59$; $L_\infty = 2535$, $k = 0.51$, $t_0 = -0.68$); back-calculation 3 ($L_\infty = 2605$, $k = 0.48$, $t_0 = -0.92$; $L_\infty = 2543$, $k = 0.49$, $t_0 = -1.00$) LJFL.

Observed LJFLs fitted to the standard VBGC resulted in the fastest growth rates for both sexes, and slower growth and larger asymptotic sizes were predicted by back-calculation models (Figure 8, Table 4). Significant (ARSS; $p < 0.001$) sex-specific differences in growth were detected in the observed growth model, so females and males were modelled separately. Back-calculation 3 and the observed VBGC provided the most parsimonious fit (lowest residual sum of squares) to LJFL-at-age data for females and males. Growth models predicted that both sexes reached 71–84% of asymptotic length during the first 2 years of life.

Length at daily age (Table 2) was fitted to a Gompertz regression model ($r^2 = 0.92$; $p < 0.001$; Table 3). There were no significant differences in daily growth between sexes. The model predicted a length of 1289 ± 204 mm LJFL at the end of the first six months of life. Instantaneous growth rates predicted by the regression model were 3.1 mm d^{-1} at 6 months (0.24% LFJL per day) and 1.5 mm d^{-1} at 12 months (0.09% LJFL per day). Striped marlin grew at a mean rate of 2.5 ± 0.7 mm per day between the ages of 130 d (3.7 mm d^{-1}) and 365 d (1.5 mm d^{-1}). Length at age 0.5 years (1289 mm LJFL) was incorporated in all VBGCs. The

LJFL-at-age 1 (1710 ± 228 mm) estimated from otolith microincrements was not different from the mean observed LJFL-at-age 1 (1703 ± 108 mm) determined from fin-spine annulus counts (Table 4).

Discussion
Age validation
This study represents the first evidence of yearly periodicity of annulus formation in fin-spines and daily periodicity of microincrements in otoliths of striped marlin. Time was not measured with absolute accuracy, so the methods are considered as semidirect or indirect age validation and should be treated accordingly (Campana, 2001; Panfili *et al.*, 2002). Yearly annulus periodicity matched results from an oxytetracycline-injected and recaptured black marlin (*Makaira indica*; Speare, 2003), and other indirect evidence from several species of billfish (Chiang *et al.*, 2004; DeMartini *et al.*, 2007). Fin-spines are certainly useful structures for age estimation of billfish, but interpretation of annuli remains complicated by vascular erosion of the core and by the presence of false increments.

The MIA revealed a single annulus formed each year in the fin-spines of striped marlin. Narrow translucent zones completed formation during the austral spring and early summer (months 10–12). The observation of a complete annulus in immature striped marlin sampled during the spawning season indicated that annulus deposition may not be related directly to spawning activity. Studies on sailfish (*Istiophorus platypterus*; Chiang *et al.*, 2004), swordfish (DeMartini *et al.*, 2007), and bigeye tuna (*Thunnus obesus*; Sun *et al.*, 2001) have related annual translucent zone completion to late spring or summer, which typically coincides with spawning activity.

Identification of false subannual increments in fin-spines suggests that a variety of factors may contribute to the formation of translucent zones. This issue warrants careful attention in future fin-spine age-determination studies on pelagic fish. False annuli have been documented in fin-spine sections of other pelagic fish, including billfish, but the underlying mechanisms influencing formation have not been well described (Hill *et al.*, 1989; Speare, 2003; Santiago and Arrizabalaga, 2005). For albacore tuna (*Thunnus alalunga*), two annuli are laid down during the first year of life, one believed to form during a feeding migration and the other over winter (Santiago and Arrizabalaga, 2005). Although a similar pattern was observed in young striped marlin, the causes of false-increment formation and its persistence in older age groups remain unknown.

Given the large maximum size of striped marlin sampled in this study, age estimates suggest that it is rare for individual fish in the SWPO to reach ages beyond 7 or 8.5 years for males and females, respectively. These estimates of maximum age were within the range of 6–12 years reported previously (Koto, 1963; Skillman and Yong, 1976; Davie and Hall, 1990; Melo-Barrera *et al.*, 2003; Kopf *et al.*, 2005). However, the observed maximum age may not be an accurate representation of maximum longevity. Conventional tags deployed on other billfish have been recovered after 10–17 years, though the maximum time at liberty for striped marlin is <3 years (Prince *et al.*, 1986; Ortiz *et al.*, 2003).

Daily periodicity of otolith microincrements was corroborated by back-calculating hatch dates, which matched the known spawning period (Hanamoto, 1977; Kopf, 2010). Otolith microstructure was indistinguishable from previous descriptions of appearance

Table 4. Length-at-age (LJFL, mm) of striped marlin ($n = 374$) in the SWPO predicted by the standard VBGC fitted to observed and back-calculated lengths.

Age (years)	n[a]	Obs.	Back calc. 1	Back calc. 2	Back calc. 3	n[a]	Obs.	Back calc. 1	Back calc. 2	Back calc. 3
			Female					**Male**		
0.5	9	1 316	1 113	1 095	1 291	8	1 353	1 149	1 141	1 323
1	4	1 640	1 422	1 428	1 573	3	1 665	1 441	1 453	1 588
1.5	0	1 880	1 668	1 687	1 794	14	1 888	1 674	1 695	1 795
2	14	2 057	1 864	1 887	1 968	48	2 047	1 861	1 883	1 958
2.5	10	2 189	2 020	2 042	2 105	13	2 159	2 011	2 029	2 085
3	29	2 286	2 144	2 163	2 212	55	2 240	2 131	2 142	2 184
3.5	24	2 359	2 243	2 257	2 296	24	2 297	2 227	2 230	2 262
4	31	2 412	2 321	2 329	2 362	8	2 338	2 304	2 298	2 323
4.5	18	2 452	2 384	2 385	2 414	7	2 366	2 366	2 351	2 371
5	9	2 481	2 434	2 429	2 455	8	2 387	2 416	2 393	2 408
5.5	11	2 503	2 473	2 463	2 487	3	2 402	2 455	2 424	2 437
6	4	2 519	2 505	2 489	2 513	1	2 412	2 487	2 449	2 460
6.5	2	2 531	2 530	2 510	2 532	0	2 420	2 513	2 468	2 478
7	3	2 540	2 550	2 526	2 548	1	2 425	2 533	2 483	2 492
7.5	3	2 546	2 566	2 538	2 560					
8	4	2 551	2 579	2 547	2 570					
8.5	2	2 555	2 589	2 555	2 577					

Significant ($p < 0.05$) sex-specific differences in growth were detected in the observed and back calculation 3 models.
[a]The sex of four fish was not determined.

and size in other billfish (Prince et al., 1991; Luthy et al., 2005; Sponaugle et al., 2005), and in species where daily periodicity has been validated (Campana and Neilson, 1985; Kayama et al., 2007). Using the same methods employed in this investigation, Speare (2003) reported an underestimate of daily age in an oxytetracycline-injected and recaptured black marlin. The potential for non-daily microincrement periodicity, or age underestimation, has been refuted statistically herein for striped marlin <1710 mm LJFL.

Otolith daily microincrements corroborated the age at first annulus formation. DeMartini et al. (2007) first combined otolith daily microincrement counts with annulus measurements to verify first annulus formation in fin-spines of swordfish. A variation in this methodology proved useful in the present investigation, but was subject to decreasing precision with increasing body size and age. Despite the relatively high APE of 7.5%, the precision in number of days (34 ± 36 d) was considered satisfactory for confirming annual age estimates derived from fin-spines. Increasingly narrow microincrements limited daily estimates of age in striped marlin to fish <436 d. Using scanning electron microscopy, daily microincrement readings have been observed in sections of otoliths from black marlin up to 1012 d (Speare, 2003), swordfish up to 720 d (DeMartini et al., 2007), and blue marlin up to 495 d (Prince et al., 1991).

Growth

Growth in length of striped marlin ranks among the fastest of all bony fish and was particularly rapid during the first 2 years of life. The success of billfish and large-bodied tuna (*Thunnus* spp.) has been attributed in part to their ability to deliver oxygen and metabolic substrata to tissues at a high rate more akin to mammals than poikilothermic fish (Carey et al., 1971; Davie, 1990; Graham and Dickson, 2004). One of the advantages of this high-performance physiology is a rapid rate of tissue turnover that facilitates equally rapid rates of somatic growth (Brill, 1996). We hypothesize that rapid juvenile growth and large maximum body size are selected for in open-ocean fish because of the long distances between feeding and spawning habitats and an absence of physical structure suitable for juveniles to avoid predation. DeMartini et al. (2007) further postulated that rapid growth of pelagic fish represents the outcome of selection for body length, because it affects swimming speed directly.

The maximum absolute growth rate in length reported for any bony fish comes from an estimate of 16.6 mm d^{-1} in a 390 mm LJFL blue marlin (Prince et al., 1991). The smallest fish available for daily growth examination in the present study was 990 mm LJFL, so direct comparison with the blue marlin was not possible. However, the growth rate of striped marlin at age 1 (1.5 mm d^{-1}) was identical to that of blue marlin at the same age (Prince et al., 1991). Growth rates between 1 and 6 mm d^{-1} are common for pelagic fish during the first few months of life (Uchiyama et al., 1986; Megalofonou et al., 1995; Luthy et al., 2005; Sponaugle et al., 2005). Unlike most pelagic fish, however, striped marlin maintained an accelerated rate of growth in body length of 1.5–3.1 mm d^{-1} after 6 months.

There is no way to determine which of the four models examined provided the most biologically accurate description of striped marlin growth. Back-calculation methods may result in biased estimates of growth (Campana, 1990; Francis, 1990), and the use of direct observations may be influenced by fisheries size selectivity (Ricker, 1975). The sex-specific standard VBGC fitted to observed LJFL and back-calculation 3 provided the best statistical fits to describing the length−age relationship. However, back-calculation models 1 and 2 resulted in asymptotic lengths closest to the observed maximum size and also provided the lowest LJFL-at-age 1. Different rates of growth between sexes after ages 2−3 coincided roughly with the age at sexual maturity (Kopf, 2010). Sex-specific differences in growth were consistent with hypotheses suggesting that larger female body size is the result of fecundity selection (Blanckenhorn, 2000).

If fisheries size-selectivity resulted in growth overestimation of the first year class, then back-calculation model 1 or 2 may provide
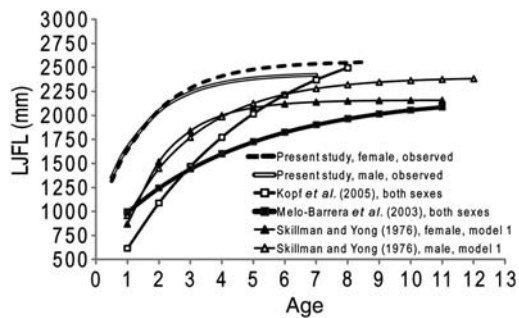
Figure 9. Comparison of the standard VBGCs and parameters estimated for striped marlin: present study, female, observed ($L_\infty = 2565$, $k = 0.60$, $t_0 = -0.70$); present study, male, observed ($L_\infty = 2438$, $k = 0.68$, $t_0 = -0.69$); Kopf *et al.* (2005), both sexes ($L_\infty = 2565$, $k = 0.60$, $t_0 = -0.70$); Melo-Barrera *et al.* (2003), both sexes ($L_\infty = 2565$, $k = 0.60$, $t_0 = -0.70$); Skillman and Yong (1976), female, model 1 ($L_\infty = 2565$, $k = 0.60$, $t_0 = -0.70$); Skillman and Yong (1976), male, model 1 ($L_\infty = 2565$, $k = 0.60$, $t_0 = -0.70$). *FL* reported by Skillman and Yong (1976) was converted to LJFL using the equations FL = a LJFL + b; female, $a = 1.067$, $b = 192.85$; male, $a = 1.021$, $b = 319.35$ (Kopf, 2010).

a better description of "true growth" (Ricker, 1975), compared with other models. It seems probable that fisheries size selectivity in the present study caught the fastest-growing young striped marlin. This species starts to recruit to commercial longline fishing gear at ~1000 mm LJFL (Nakamura, 1985), but fish of that size are rarely caught in commercial longline fisheries of the SWPO (Kopf, 2010). Juveniles are restricted primarily to tropical waters, which were less intensively sampled than subtropical areas in the present study. Evidence of Lee's phenomenon (Lee, 1912), as a consequence of fisheries size selectivity, was also apparent because all estimates of back-calculated LJFL-at-age 1 were smaller than observed LJFL-at-age 1 (Panfili *et al.*, 2002).

Growth of striped marlin in the present study (Figure 9) differed most from previous fin-spine age-determination studies conducted in México (Melo-Barrera *et al.*, 2003) and New Zealand (Kopf *et al.*, 2005) and was most similar to length frequency analyses conducted in Hawaii (Skillman and Yong, 1976) and the western North Pacific (Koto, 1963). The main difference between growth curves was a larger LJFL-at-age 1 in the present investigation than in previous studies. Earlier studies on striped marlin ranged from 615 to 994 mm LJFL, compared with the 1422 mm (back-calculation 1; female) to 1674 mm LJFL (observed; male) in the present investigation. Koto (1963) did not fit a VBGC, but estimated a growth rate of 350 mm between putative age groups 1 and 2. The present study estimated an average growth rate of ~366 mm over the same period. The LJFL-at-age 1 reported here was greater than that of some studies conducted on other istiophorid billfish (Hill *et al.*, 1989; Chiang *et al.*, 2004), but consistent with growth estimates from earlier studies corroborated by otolith daily microincrements and tag recaptures (Prince *et al.*, 1991; Hoolihan, 2006). Speare (2003) estimated that an oxytetracycline-injected and recaptured black marlin of ~20 kg or ~1313 mm LJFL would be 474-d old, closest to the results of back-calculation models 1 and 2 in the present study.

As the size-structure of striped marlin varies widely in the Pacific Ocean (Squire and Suzuki, 1990; Kopf *et al.*, 2005), region-specific growth rates would be expected. For this reason, growth estimates of striped marlin should not be used outside the region where samples were collected. It seems unlikely, however, that such divergent estimates of size-at-age (i.e. growth) between previous studies (Skillman and Yong, 1976; Melo-Barrera *et al.*, 2003; Kopf *et al.*, 2005) and the present investigation can be attributed entirely to natural variation. False annuli, which were corroborated by daily microincrement counts, were identified in fin-spine sections of striped marlin in this study, suggesting that misidentification of the first annulus led to age overestimation and growth underestimation of the first year class in at least the previous study conducted in New Zealand (Kopf *et al.*, 2005). The extent to which false increment formation has affected growth estimates in other studies remains unknown, but merits careful attention by future investigators. Further analyses using comparable age-determination techniques are needed to evaluate basin-scale differences in growth.

Conclusions

The development of a growth model for striped marlin in the SWPO represents an important step towards reducing the uncertainties and assumptions of previous stock assessments. Historical declines in abundance demonstrate that the species is vulnerable to overexploitation (Langley *et al.*, 2006; Brodziak and Piner, 2010), and future stock assessments need to consider several limitations of this research carefully. First, the maximum longevity of individual striped marlin remains unknown. Second, growth estimates were based on a relatively small sample of fish, when one considers the large geographic area of the SWPO. In particular, few samples were available from French Polynesia and few were available from direct observation (i.e. not back-calculated) of juveniles.

Direct validation of growth in billfish may be achieved through large-scale, long-term chemical marking programmes. Such programmes may be implemented through existing conventional tagging operations in recreational fisheries (Speare, 1992, 2003; Ortiz *et al.*, 2003). Increasing sensitivity of mass spectrometry may also provide a biochemical means of validating longevity in future age studies on billfish. In particular, it may be possible to apply bomb-radiocarbon or radiometric analyses to archived otolith cores or other calcified structures (Campana, 2001; Campana *et al.*, 2006; Kerr *et al.*, 2006). The successful long-term maintenance of billfish larvae and juveniles in captivity would provide an opportunity to measure growth directly and to investigate the apparently exceptional metabolic rate of this group of fish.

References

Beamish, R. J., and Fournier, D. A. 1981. A method for comparing the precision of a set of age determinations. Canadian Journal of Fisheries and Aquatic Sciences, 38: 982–983.

Blanckenhorn, W. U. 2000. The evolution of body size: what keeps organisms small? Quarterly Reviews in Biology, 75: 385–407.

Brill, R. W. 1996. Selective advantages conferred by the high performance physiology of tunas, billfishes and dolphin fish. Comparative Biochemistry and Physiology, 113: 3–15.

Brodziak, J., and Piner, K. 2010. Model averaging and probable status of North Pacific striped marlin, *Tetrapturus audax*. Canadian Journal of Fisheries and Aquatic Sciences, 67: 793–805.

Bromhead, D., Pepperell, J., Wise, B., and Findlay, J. 2004. Striped marlin: biology and fisheries. Final Report to the Australian Fisheries Management Authority and the Fisheries Research Fund. Bureau of Rural Sciences, Canberra, Australia.

Brothers, E. B., Prince, E. D., and Lee, D. W. 1983. Age and growth of young-of-the-year bluefin tuna, *Thunnus thynnus*, from otolith microstructure. *In* Proceedings of the International Workshop on Age Determination of Oceanic Pelagic Fishes: Tunas, Billfish, and Sharks, pp. 49–59. Ed. by E. D. Prince, and L. M. Pulos. NOAA Technical Report, NMFS 8.

Campana, S. E. 1990. How reliable are growth back-calculations based on otoliths? Canadian Journal of Fisheries and Aquatic Sciences, 47: 2219–2227.

Campana, S. E. 2001. Accuracy, precision and quality control in age determination, including a review of the use and abuse of age validation methods. Journal of Fish Biology, 59: 197–242.

Campana, S. E., Jones, C., McFarlane, G. A., and Myklevoll, S. 2006. Bomb dating and age validation using the spines of spiny dogfish (*Squalus acanthias*). Environmental Biology of Fishes, 77: 327–336.

Campana, S. E., and Neilson, J. D. 1985. Microstructure of fish otoliths. Canadian Journal of Fisheries and Aquatic Sciences, 42: 1014–1032.

Carey, F. G., Teal, J. M., Kanwisher, J. W., Lawson, K. D., and Beckett, J. S. 1971. Warm bodied fish. American Zoologist, 11: 135–143.

Chen, Y., Jackson, D. A., and Harvey, H. H. 1992. A comparison of von Bertalanffy and polynomial functions in modelling fish growth data. Canadian Journal of Fisheries and Aquatic Sciences, 49: 1228–1235.

Chiang, W. C., Sun, C. L., Yeh, S. Z., and Su, W. C. 2004. Age and growth of sailfish (*Istiophorus platypterus*) in waters off eastern Taiwan. Fishery Bulletin US, 102: 251–263.

Collette, B. B., McDowell, J., and Graves, J. 2006. Phylogeny of recent billfishes (Xiphioidei). Bulletin of Marine Science, 79: 455–468.

Dalzell, P., and Boggs, C. 2003. Pelagic fisheries catching blue and striped marlins in the US western Pacific islands. Marine and Freshwater Research, 54: 419–424.

Davie, P. S. 1990. Pacific Marlins: Anatomy and Physiology. Simon Print, Palmerston North, New Zealand.

Davie, P. S., and Hall, I. 1990. Potential of dorsal and anal spines and otoliths for assessing age structure of the recreational catch of striped marlin in New Zealand. *In* Proceedings of the Second International Billfish Symposium, pp. 287–294. Ed. by R. H. Stroud. Kailua-Kona, Hawaii.

DeMartini, E. E., Uchiyama, J. H., Humphreys, R. L., Sampaga, J. D., and Williams, H. A. 2007. Age and growth of swordfish (*Xiphias gladius*) caught by the Hawaii-based pelagic longline fishery. Fishery Bulletin US, 105: 356–367.

Domeier, M. L. 2006. An analysis of Pacific striped marlin (*Tetrapturus audax*) horizontal movement patterns using pop-up satellite archival tags. Bulletin of Marine Science, 79: 811–825.

Drew, K., Die, D. J., and Arocha, F. 2006. Understanding vascularization in fin spines of white marlin (*Tetrapturus albidus*). Bulletin of Marine Science, 79: 847–852.

Ehrhardt, N. M. 1992. Age and growth of swordfish, *Xiphias gladius*, in the northwestern Atlantic. Bulletin of Marine Science, 50: 292–301.

Francis, R. I. C. C. 1990. Back-calculation of fish length: a critical review. Journal of Fish Biology, 36: 883–902.

Graham, J. B., and Dickson, K. A. 2004. Tuna comparative physiology. Journal of Experimental Biology, 207: 4015–4024.

Hanamoto, E. 1977. Fishery oceanography of striped marlin. 2. Spawning activity of the fish in the southern Coral Sea. Bulletin of the Japanese Society of Scientific Fisheries, 43: 1279–1286.

Hill, K. T., Cailliet, G. M., and Radtke, R. L. 1989. A comparative analysis of growth zones in four calcified structures of Pacific blue marlin, *Makaira nigricans*. Fishery Bulletin US, 87: 829–843.

Holdsworth, J., Saul, P., and Browne, G. 2003. Factors affecting striped marlin catch rate in the New Zealand recreational fishery. Marine and Freshwater Research, 54: 473–481.

Holdsworth, J. C., Sippel, T. J., and Block, B. A. 2009. Near real time satellite tracking of striped marlin (*Kajikia audax*) movements in the Pacific Ocean. Marine Biology, 156: 505–514.

Holland, K. 2003. A perspective on billfish biological research and recommendations for the future. Marine and Freshwater Research, 54: 343–347.

Hoolihan, J. P. 2006. Age and growth of Indo-Pacific sailfish, *Istiophorus platypterus*, from the Arabian Gulf. Fisheries Research, 78: 218–226.

ISC (International Scientific Committee for Tuna and Tuna-like Species in the North Pacific Ocean). 2010. Report of the Billfish Working Group Workshop, 12–13 July 2010, Victoria, BC, Canada.

Jones, C. M. 2000. Fitting growth curves to retrospective size-at-age data. Fisheries Research, 46: 123–129.

Kayama, S., Tanabe, T., Ogura, M., Okuhara, M., Tanaka, S., and Watanabe, Y. 2007. Validation of daily ring formation in sagittal otoliths of late juvenile skipjack tuna *Katsuwonus pelamis*. Fisheries Science, 73: 958–960.

Kerr, L. A., Andrews, A. H., Cailliet, G. M., Brown, T. A., and Coale, K. H. 2006. Investigations of $\Delta^{14}C$, $\delta^{13}C$, and $\delta^{15}N$ in vertebrae of white shark (*Carcharodon carcharias*) from the eastern North Pacific Ocean. Environmental Biology of Fishes, 77: 337–353.

Kopf, R. K. 2010. Age, growth, and reproductive dynamics of striped marlin, *Kajikia audax* in the southwest Pacific Ocean. PhD thesis, Charles Sturt University, Australia. 235 pp.

Kopf, R. K., and Davie, P. S. 2011. Fin-spine selection and section level influence potential age estimates of striped marlin (*Kajikia audax*). Copeia, 2011: 153–160.

Kopf, R. K., Davie, P. S., and Holdsworth, J. C. 2005. Size trends and population characteristics of striped marlin, *Tetrapturus audax* caught in the New Zealand recreational fishery. New Zealand Journal of Marine and Freshwater Research, 39: 1145–1156.

Kopf, R. K., Drew, K., and Humphreys, R. L. J. 2010. Age estimation of billfishes (*Kajikia* spp.) using fin spine cross-sections: the need for an international code of practice. Aquatic Living Resources, 23: 13–23.

Koto, T. 1963. Some considerations on the growth of marlins, using size frequencies in commercial catches. 3. Attempts to estimate the growth of striped marlin, *Tetrapturus audax* (Philippi) in the western North Pacific Ocean. Report of the Nankai Bulletin of Regional Fisheries Research Laboratory, 17: 63–85.

Langley, A., Molony, B., Bromhead, D., Yokawa, K., and Wise, B. 2006. Stock assessment of striped marlin (*Tetrapturus audax*) in the southwest Pacific Ocean. Western and Central Pacific Fisheries Commission Document, WCPFC-SC2-2006/SA WP-6.

Lee, R. M. 1912. An investigation into the methods of growth determination in fishes. Publicacion de Circonstance Conseil International pour l'Exploration de la Mer, s1: 3–34.

Luthy, S. A., Serafy, J. E., Cowen, R. K., Denit, K. L., and Sponaugle, S. 2005. Age and growth of larval Atlantic sailfish, *Istiophorus platypterus*. Marine and Freshwater Research, 56: 1027–1035.

McDowell, J. R., and Graves, J. E. 2008. Population structure of striped marlin (*Kajikia audax*) in the Pacific Ocean based on analysis of microsatellite and mitochondrial DNA. Canadian Journal of Fisheries and Aquatic Sciences, 65: 1307–1320.

Megalofonou, P., Dean, J. M., De Metrio, G., Wilson, C., and Berkeley, S. 1995. Age and growth of juvenile swordfish, *Xiphias gladius* Linnaeus, from the Mediterranean Sea. Journal of Experimental Marine Biology and Ecology, 188: 79–88.

Melo-Barrera, F. N., Felix Uraga, R., and Quinonez Velazquez, C. 2003. Growth and length–weight relationship of the striped marlin, *Tetrapturus audax* (Pisces: Istiophoridae), in Cabo San Lucas, Baja California Sur, Mexico. Ciencias Marinas, 29: 305–313.

Nakamura, I. 1985. Billfishes of the world. An annotated and illustrated catalogue of marlins, sailfishes, spearfishes and swordfishes known to date. FAO Species Catalogue, 5: 40–42.

Ortiz, M., Prince, E., Serafy, J., Holts, D., Davy, K., Pepperell, J., Lowry, M., *et al.* 2003. Global overview of the major constituent-based billfish tagging programs and their results since 1954. Marine and Freshwater Research, 54: 489–507.

Panfili, J., de Pontual, J., Troadec, J., and Wright, P. J. 2002. Manual of Fish Sclerochronology. Ifremer–IRD coedition, Brest, France.

Prince, E. D., Lee, D. W., and Berkeley, S. A. 1988. Use of marginal increment analysis to validate the anal spine method for ageing Atlantic swordfish and other alternatives for age determination. ICCAT Collective Volume of Scientific Papers, 27: 194–201.

Prince, E. D., Lee, D. W., Wilson, C. A., and Dean, J. M. 1986. Longevity and age validation of a tag-recaptured Atlantic sailfish, *Istiophorus platypterus*, using dorsal spines and otoliths. Fishery Bulletin US, 84: 493–502.

Prince, E. D., Lee, D. W., Zweifel, J. R., and Brothers, E. B. 1991. Estimating age and growth of young Atlantic blue marlin *Makaira nigricans* from otolith microstructure. Fishery Bulletin US, 89: 441–459.

Radtke, R. L. 1983. Istiophorid otoliths: extraction, morphology and possible use as ageing structures. *In* Proceedings of the International Workshop on Age Determination of Oceanic Pelagic Fishes: Tunas, Billfish, and Sharks, pp. 123–129. Ed. by E. D. Prince, and L. M. Pulos. NOAA Technical Report, NMFS 8.

Ralston, S., and Williams, H. A. 1988. Numerical integration of daily growth increments: an efficient means of ageing tropical fishes for stock assessment. Fishery Bulletin US, 87: 1–6.

Rasband, W. S. 1997–2008. ImageJ, ver 1.32. US National Institutes of Health, Bethesda, MD.

Revill, A. T., Young, J. W., and Lansdell, M. 2009. Stable isotopic evidence for trophic grouping and bioregionalization of predators and their prey in oceanic waters off eastern Australia. Marine Biology, 156: 1432–1793.

Richards, F. J. 1959. A flexible growth function for empirical use. Journal of Experimental Botany, 10: 290–300.

Ricker, W. E. 1975. Computation and interpretation on biological statistics of fish population. Bulletin of the Fisheries Research Board of Canada, 191: 215–218.

Santiago, J., and Arrizabalaga, H. 2005. An integrated growth study for North Atlantic albacore (*Thunnus alalunga* Bonn. 1788). ICES Journal of Marine Science, 62: 740–749.

SAS Institute. 1990. SAS/STAT User's Guide, Version 6, 4th edn. Volume 2. SAS Institute, Cary, NC.

Sippel, T. J., Davie, P. S., Holdsworth, J. C., and Block, B. A. 2007. Striped marlin (*Tetrapturus audax*) movements and habitat utilization during a summer and autumn in the Southwest Pacific Ocean. Fisheries Oceanography, 16: 459–472.

Skillman, R. A., and Yong, M. Y. Y. 1976. Von Bertalanffy growth curves for striped marlin *Tetrapturus audax* and blue marlin *Makaira nigricans* in the central North Pacific Ocean. Fishery Bulletin US, 74: 553–566.

Speare, P. 1992. A technique for tetracycline injecting and tagging billfish. Bulletin of Marine Science, 51: 197–203.

Speare, P. 2003. Age and growth of black marlin, *Makaira indica*, in east coast Australian waters. Marine and Freshwater Research, 54: 307–314.

Sponaugle, S., Denit, K. L., Luthy, S. A., Serafy, J. E., and Cowen, R. K. 2005. Growth variation in larval *Makaira nigricans*. Journal of Fish Biology, 66: 822–835.

Squire, J. L., and Suzuki, Z. 1990. Migration trends of striped marlin (*Tetrapturus audax*) in the Pacific Ocean. *In* Proceedings of the Second International Billfish Symposium, pp. 67–80. Ed. by R. H. Stroud. Kailua-Kona, Hawaii.

Sun, C. L., Huang, C. L., and Yeh, S-Z. 2001. Age and growth of the bigeye tuna, *Thunnus obesus*, in the western Pacific Ocean. Fishery Bulletin US, 99: 502–509.

Uchiyama, J. H., Burch, R. K., and Kraul, S. A. 1986. Growth of dolphins, *Coryphaena hippurus* and *C. equiselis*, in Hawaiian waters as determined by daily increments on otoliths. Fishery Bulletin US, 84: 186–191.

von Bertalanffy, L. 1938. A quantitative theory of organic growth. Human Biology, 10: 181–213.

Yatomi, H. 1990. Potential problem in estimating the ages of striped marlin using dorsal fin spines. *In* Proceedings of the Second International Billfish Symposium, pp. 317–321. Ed. by R. H. Stroud. Kailua-Kona, Hawaii.

Zar, J. H. 1999. Biostatistical Analysis, 4th edn. Prentice-Hall, Upper Saddle River, NJ.